LBL-33652
UC-413
Preprint

Lawrence Berkeley Laboratory
UNIVERSITY OF CALIFORNIA

Submitted to Physical Review C

Electron-Capture Decay of ^{100}Tc and the Double β Decay of ^{100}Mo

A. Garcia, Y.D. Chan, M.T.F. da Cruz, R.M. Larimer, K.T. Lesko, E.B. Norman, R.G. Stokstad, F.E. Wietfeldt, I. Zlimen, D.M. Moltz, J. Batchelder, T.J. Ognibene and M.M. Hindi

February 1993

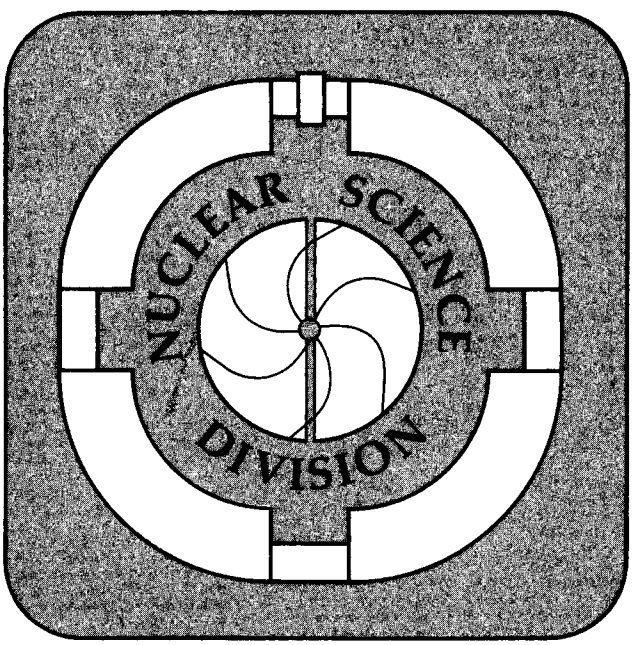

Prepared for the U.S. Department of Energy under Contract Number DE-AC03-76SF00098

DISCLAIMER

LBL - 33652

Electron-Capture Decay of ^{100}Tc and the Double β Decay of ^{100}Mo

A. Garcia, Y.D. Chan, M.T.F. da Cruz,† R.M. Larimer, K.T. Lesko, E.B. Norman, R.G. Stokstad, F.E. Wietfeldt, I. Zlimen,‡ D.M. Moltz, J. Batchelder, T.J. Ognibene

Nuclear Science Division, Lawrence Berkeley Laboratory, Berkeley, CA. 94720

M.M. Hindi

Physics Department, Tennessee Technological University, Cookeville, TN 38505

Nuclear Science Division, Lawrence Berkeley Laboratory
University of California, Berkeley, California 94720, USA

February, 1993

This work was supported by the Director, Office of Energy Research Division of Nuclear Physics of the Office of High Energy and Nuclear Physics of the U.S. Department of Energy under Contract DE-AC03-76SF00098

Electron-Capture Decay of ^{100}Tc and the Double-β Decay of ^{100}Mo

A. García, Y-D Chan, M.T.F. da Cruz,† R.M. Larimer, K.T. Lesko, E.B. Norman, R.G. Stokstad, F.E. Wietfeldt, I. Žlimen,‡ D.M. Moltz, J. Batchelder, T.J. Ognibene

Nuclear Science Division, Lawrence Berkeley Laboratory, Berkeley, CA 94720

M.M. Hindi

Physics Department, Tennessee Technological University, Cookeville, TN 38505.

Abstract

We have measured the electron-capture decay branch of ^{100}Tc to be $(1.8 \pm 0.9) \times 10^{-3}$ %, from which we deduce $\log ft = 4.40^{+0.18}_{-0.30}$. This indicates that a two-step process connecting only the ground states of ^{100}Mo-^{100}Tc-^{100}Ru can account for the measured 2ν double-β decay rate of ^{100}Mo.

I. MOTIVATION

In order to interpret the results of experiments on double-β decay one needs to understand the relevant nuclear physics. In this respect, there is a longstanding discrepancy between calculated and measured 2ν decay rates [1]. The case of ^{100}Mo promises to be a benchmark for testing nuclear calculations. The 2ν decay rate to the ground state of ^{100}Ru has been recently measured: $t_{1/2} = (1.16^{+0.34}_{-0.08}) \times 10^{19}$y [2] and $t_{1/2} = (1.15^{+0.30}_{-0.20}) \times 10^{19}$y [3]. One can compare these to an estimation of the contribution of the virtual transition via only the ground state of ^{100}Tc to the 2ν decay rate (see Fig. 1), making use of the equation [4]:

$$t_{1/2}^{-1} = G^{2\nu}(E_0, Z)|M_{\rm GT}^{2\nu}|^2. \tag{1}$$

Here $G^{2\nu}(E_0, Z)$ results from lepton phase space integration and $M_{\rm GT}^{2\nu}$ contains the nuclear matrix element. In our naive calculation we estimate the latter as:

$$M_{\rm GT}^{2\nu} = \frac{<^{100}\,\mathrm{Ru}||\sigma\tau^+||^{100}\mathrm{Tc(g.s.)}><^{100}\,\mathrm{Tc(g.s.)}||\sigma\tau^+||^{100}\mathrm{Mo}>}{(Q_{\rm EC} + Q_{\beta^-})/2} \tag{2}$$

The β^- log ft value of ^{100}Tc to the g.s. of ^{100}Ru is known from the half-life and decay branch to the g.s. [5], but the electron-capture (EC) decay branch is not known. If we assume it to be similar to corresponding transitions in the neighboring nuclei ^{98}Zr and ^{102}Mo, *i.e.*, log ft=4.2, we obtain $t_{1/2} \approx 5.4 \times 10^{18}$ y. This shows that the contribution from the ground state of ^{100}Tc could exceed the total rate, thus requiring the higher excitation energy levels to interfere destructively. A similar argument was presented by Abad *et al.* [6] who showed that this situation could be common to all $0^+ \rightarrow 0^+$ double-β-decaying nuclei in which the ground state of the intermediate nucleus has $J^\pi = 1^+$. However, it could be argued that some particular cancellation is taking place in the EC matrix element and that our estimate of log ft=4.2 is an overprediction of the EC decay rate. The expected decay branch for the EC decay corresponding to log ft=4.2 is $\approx 2.9 \times 10^{-3}$%. In the following section we describe an experiment we performed in order to measure the EC decay rate of ^{100}Tc.

II. EXPERIMENT

A. Production of ^{100}Tc and Experimental Set-Up

We produced ^{100}Tc by means of the ^{100}Mo(p,n) reaction using a 9 MeV proton beam from the 88-Inch Cyclotron at Lawrence Berkeley Laboratory. The beam impinged on a stack of six self-supporting ^{100}Mo targets. Each target was enriched to 97.4% isotopic purity and was $\approx$500 μg/cm^2 thick. A He-jet system was used to transport the ^{100}Tc to a remote shielded counting station. This was important because Mo x rays, which constitute the signature for the EC decay of ^{100}Tc, are profusely generated by particle or photon excitation of the Mo targets.

The radioactivity in the He jet was deposited on a polypropylene tape which was moved every 30 seconds by a computer tape drive unit to position the radioactivity in the center of our counting station, which is shown in Fig. 2. (In what follows we will refer to this mode as 'fast-cycle'). We typically obtained a deposition rate of $\approx 5\times10^4$ ^{100}Tc atoms/s from the He jet onto the tape. We counted the EC decays by detecting Mo x rays (E_x = 17.4 keV) using a Ge planar detector, 2 cm in diameter and 0.5 cm thick. Because these x rays are not accompanied by the emission of either γ rays or β rays, whereas the β^- decay of ^{100}Tc produces coincident γ's and β's, we used two additional detectors as vetos to reduce the background. The tape was threaded through a plastic scintillating detector, which was located in front of the Ge detector. A 33-cm diameter, 26-cm long segmented annular NaI detector surrounded the Ge and plastic detectors. Every time there was a signal in the Ge detector we recorded the energy and timing signals of the plastic scintillator and NaI detectors. In order to measure the half-life corresponding to the Mo x ray, we also recorded, for every event, the time interval between the start of the counting cycle, *i.e.*, positioning of the fresh radioactivity in place, and the detection of a signal in the Ge detector. This was done by recording the readout of a scaler that was zeroed each time the radioactivity was positioned in the counting station (every $\approx$30 seconds) and incremented by a ($\approx$30 Hz.)

pulser.

B. Results

Fig. 3 shows the spectra taken with the Ge detector. The raw spectrum in Fig. 3a shows the 540 keV-591 keV cascade from the β^- decays to ^{100}Ru*, on top of a continuum of 3.2-MeV-endpoint βs from decays to ^{100}Ru(g.s.). In addition, we observe 511 keV γ rays from β^+-annihilation and 440-keV γ rays from ^{23}Mg. We speculate that the latter is produced due to Na contamination of the targets. At very low energies one notices a rise in the background due to β-bremsstrahlung radiation. The EC decay can be detected by measuring the Mo $K\alpha$ x ray which is emitted with 57% probability. In order to improve our sensitivity to x rays we used the plastic scintillator detector to reduce the low energy background by vetoing any event that produced a signal in the scintillator. In addition, we vetoed any event that produced a signal in the annular NaI. This suppressed the Compton background and was essential in reducing the effect of Tc contaminants, as we will show below. Fig. 3b shows the low energy portion of the raw and plastic-plus-NaI vetoed spectra.

Finally, Fig. 4 presents a fit to the vetoed spectrum, which we used to estimate the area of the Mo $K\alpha$ x ray peak. We fixed the relative intensities of the $K\alpha_1$, $K\alpha_2$, $K\beta_1$, $K\beta_2$, and $K\beta_3$, for the x rays corresponding to each element, according to the tables of ref. [7] and taking into account the measured relative efficiencies. In this way we obtained 1424 ± 334 for the area of the $K\alpha$ Mo x ray peak.

C. Efficiency of Ge detector

In order to calculate the EC decay branch we determined the relative detection efficiencies in the following way:

1. We first performed a relative measurement using a ^{96}Tc source that we prepared during our experiment, produced by ^{96}Mo (p, n) due to the impurity of our target. This source

produces Mo x rays and γ rays of 778, 812, and 850 keV with known relative intensities [5], and this allowed us to calculate the ratios $\frac{\eta(\text{Mo x ray})}{\eta(778\text{ keV})}$, $\frac{\eta(\text{Mo x ray})}{\eta(812\text{ keV})}$, and $\frac{\eta(\text{Mo x ray})}{\eta(850\text{ keV})}$, where $\eta(E)$ is the photopeak efficiency at energy E.

2. We then measured the absolute efficiency in the 100 keV-1300 keV range using standard calibrated γ-ray sources of ^{57}Co, ^{137}Cs and ^{60}Co. We fitted the data to a curve of the form:

$$\eta(\%) = a_1 \times (E_\gamma)^{a_2} \tag{3}$$

The latter measurements together with the fit are shown in Fig. 5.

In this way we determined the ratios $\frac{\eta(\text{Mo x ray})}{\eta(540\text{ keV})} = 19.0 \pm 1.4$, and $\frac{\eta(\text{Mo x ray})}{\eta(140\text{ keV})} = 1.4 \pm 0.1$ that we need for calculating the EC decay branch, and the contribution of contaminants, respectively, as discussed below.

D. Contaminants

A potential source of background arises from Tc isotopes that decay by EC emitting Mo x rays in a large fraction of their decays and from Nb isotopes that can β^- decay and emit a Mo x ray as a result of a γ-ray internal conversion. These isotopes can be produced mainly by the (p,n) and (p,α) reactions on different Mo isotopes. Table I presents the isotopic composition of our Mo targets. Because most of the produced contaminant isotopes are long-lived, we prepared a separate source by collecting radioactivity on a fixed tape location for 2 hours and then collected γ-ray spectra for one day in 1 hour time bins. Fig. 6 shows the areas of some characteristic Tc isotope γ rays as a function of time. The corresponding fits were used to deduce the amount of contaminants present in our experiment, which are listed in Table II. The 140.5-keV γ ray from ^{99}Tc^m is visible in both the 'fast-cycle' experiment (Fig. 3) and in the 2-hour-source counting (Fig. 6). We therefore used the 140.5-keV γ ray as a normalization. We first calculated the ratio of the rate of deposition of contaminant atoms on the tape (atoms per second) to the rate of deposition of ^{99}Tc using the 2-hour-source

data, and then, based on the known decay scheme of each isotope, deduced the number of $K\alpha$ Mo x rays that should have been detected in the 'fast-cycle' experiment normalized to the number of 140.5-keV γ rays. Table II lists the deduced deposition rates of contaminant isotopes producing Mo x rays (column three) and the expected ratio of Mo x rays to ^{99}Tc 140.5-keV γ rays (column five). Because all of the Tc contaminants decay to excited states of the daughters emitting prompt γ's, the NaI veto suppressed these sources of Mo x rays. Column six indicates the fraction of Mo x rays that escaped the veto. This fraction depends on the number and energy of the γ rays emitted after the EC decay for the Tc isotopes, and on the efficiency of the plastic detector for the Nb isotopes. We measured the NaI veto efficiency using three sources of coincident γ rays.

1. A standard ^{60}Co source which produces a cascade of 1173 and 1332 keV γ rays.

2. The 2-hour-source, which after two days was almost pure ^{96}Tc. This isotope produces three γ rays in coincidence with a Mo x ray.

3. The 540- and 591-keV γ rays following the β^- decay of ^{100}Tc.

The results were slightly dependent on the γ-ray energy and we used a linear fit to the data to calculate the NaI veto efficiency for each particular γ-ray energy. In cases where there are EC decays to several daughter states, the number in column six gives the 'effective NaI vetoing efficiency', *i.e.*, the product of this number times the intensity in column four gives the percentage of decays of the particular contaminant which are accompanied by an x ray and are not vetoed by the NaI detector. Finally, column seven of Table II shows the effective contribution of each contaminant to the area of the Mo $K\alpha$ x-ray peak. Because the half-life of ^{92}Tc is rather short ($t_{1/2}$=4.4 minutes) we placed an upper limit on the flux of this contaminant by looking for the characteristic γ rays in the second Ge counter (Fig. 2).

After subtracting these contributions from the measured Mo $K\alpha$ x-ray peak area we obtain the number of Mo $K\alpha$ x rays attributable to the EC decay of ^{100}Tc:

$$A(\text{Mo x ray}) = (687 \pm 347) \tag{4}$$

E. Determination of the EC Decay Branch

The total number of ^{100}Tc decays is directly related to the area of the 540 keV peak, for which we obtain $A(540\text{ keV})=(2.48 \pm 0.05) \times 10^5$.

We calculate the EC decay branch as:

$$B(\text{EC}) = \frac{A(\text{Mo x ray})}{A(540\text{ keV})} \times \frac{\eta(540\text{ keV})}{\eta(\text{Mo x ray})} \times \frac{b.r.(540\text{ keV})}{f_K \times \omega_{K\alpha}(\text{Mo x ray})} \tag{5}$$

where $\frac{\eta(540\text{ keV})}{\eta(\text{Mo x ray})} = \frac{1}{19.0 \pm 1.4}$ is the ratio of Ge detector efficiencies and $b.r.(540\text{ keV}) = (7.0 \pm 0.7) \times 10^{-2}$ is the probability of emission of a 540 keV γ ray in a β^- decay; $f_K = 0.88$ is the fraction of EC decays that produce a vacancy in the K shell and $\omega_{K\alpha} = 0.65$ is the $K\alpha$ fluorescence yield, *i.e.*, the probability of emission of a $K\alpha$ Mo x ray per K vacancy [7]. We thus obtain:

$$B(\text{EC}) = (1.8 \pm 0.9) \times 10^{-3}\%. \tag{6}$$

This is the main result of this work. The implications are discussed in section III.

F. Half-life measurement

In order to verify the origin of the x rays we measured the corresponding half-life. Fig. 7 presents the total scaler spectrum. Note that the spectrum shows an exponential decay with a half-life roughly corresponding to ^{100}Tc($t_{1/2}$=15.8 s). Using the seven gates shown in the figure we produced seven vetoed low energy spectra that we fit in the same way as the total spectrum of Fig. 4, and obtained seven Mo $K\alpha$ x-ray peak areas that we used to measure the half-life. Fig. 8 shows the data and the best fit obtained with a fixed constant term (to account for the contribution due to contaminants) plus an exponential with free amplitude and half-life. The best fit corresponds to $t_{1/2} = 10^{+7}_{-3}$ s, which agrees with the known half-life of ^{100}Tc.

G. Ru x rays and IC and IIE in ^{100}Tc β^- decay

Our experiment allowed us to measure the number of K vacancies produced in ^{100}Ru due to internal conversion (IC) and internal ionization and excitation (IIE) in the decay of ^{100}Tc. (See ref. [8] for a recent review of the latter subject). The Ru $K\alpha$ x-ray peak is composed of three contributions: A(raw)=A(IC 540)+A(IC 591)+A(IIE). The former two come from the internal conversion of the 540 and 591 keV γ rays, and the latter from IIE in the β^- decay. Because of the small decay branch of the γ rays ($\approx$ 7 %), both contributions (IC and IIE) are roughly equal. Because the 540-keV and 591-keV are almost 100% in cascade, they appeared reduced in the NaI-vetoed Ge spectrum. The IC contribution should have the same sensitivity to the NaI Veto as the 540- and 591-keV γ rays, while 93% of the IIE contribution should not be affected (see Fig. 1). Then, the area of the Ru $K\alpha$ x-ray peak in the NaI-vetoed Ge spectrum should be:

$$A(\text{after NaI veto}) \approx A(\text{IC 540})/R(540) + A(\text{IC 591})/R(591) + A(\text{IIE}) \times 0.93 \qquad (7)$$

where we have neglected the small contribution of the IIE corresponding to the decay to the excited states that is strongly vetoed. Table III presents the measured ratios R = A(raw)/A(after NaI veto) for the Ru $K\alpha$ x-ray peak and for the 540 and 591 keV γ rays. Based on this information and assuming that the IC coefficients for the two γ rays are in the same ratio as the calculated [5] values, we obtain:

$$\frac{A(\text{IC})}{A(\text{IIE})} = 0.88 \pm 0.22. \qquad (8)$$

We now use the areas of the Ru x rays and the 540- and 591-keV γ rays measured in our experiment and obtain:

$$e_K/\gamma(540) = (4.4 \pm 0.5) \times 10^{-3} \qquad (9)$$

$$e_K/\gamma(591) = (3.5 \pm 0.5) \times 10^{-3} \qquad (10)$$

$$P_K = (6.0 \pm 0.6) \times 10^{-4}. \qquad (11)$$

Here P_K is the probability for IIE. This result is larger than the IIE probability measured for ^{99}Tc [9]: $P_K = (3.89 \pm 0.16) \times 10^{-4}$, but differences of this order of magnitude between neighboring nuclei are not rare [8]. The internal conversion values are in agreement with the calculations [5]:

$$e_K/\gamma(540) = 3.8 \times 10^{-3} \tag{12}$$

$$e_K/\gamma(591) = 3.0 \times 10^{-3}. \tag{13}$$

III. CONCLUSIONS

Our measurement of the EC decay branch of ^{100}Tc implies $\log ft = 4.40^{+0.18}_{-0.30}$, where we have used the tables of ref. [10] to calculate the factor f. This can now be used in eq. 1 to calculate the contribution of the ground state of ^{100}Tc to the 2ν double-β decay rate, to yield:

$$t_{1/2} = (8.5 \pm 4.3) \times 10^{18}\text{y}. \tag{14}$$

This confirms the guess, presented in section I, based on the $\log ft$ measured for neighboring nuclei, that the contribution of the ground state of ^{100}Tc alone, can account for the 2ν double-β decay rate of ^{100}Mo. Thus, for the case of ^{100}Mo, we have a confirmation of the 'low-lying-state-dominance hypothesis' suggested by Abad *et al.* [6]. This model also predicts a 2ν double-β-decay half-life of $(1.5 \pm 0.2) \times 10^{25}$ y, for the case of ^{128}Te, which is reasonably close to the recently measured value of $(7.7 \pm 0.4) \times 10^{24}$ y [11].

There have been essentially two different approaches to perform calculations of double-β decay rates including an explicit summation over the intermediate nucleus. The shell-model approach, with a variety of interactions, seemed [1] to overpredict the decay rates. Quasiparticle-random-phase-approximation (QRPA) calculations, on the other hand, have been shown to be able to explain the measured 2ν rates by fitting a parameter, α_1', which represents the strength of particle-particle interactions [12]. However, Griffiths and Vogel

have recently found [13] that the QRPA calculation cannot simultaneously reproduce a set of five experimental numbers in ^{100}Mo. They used the measured 2ν double-β decay rates to the g.s. [2] and 0^+ excited state of ^{100}Ru [14], the corresponding β^--decay rates from ^{100}Tc, and the EC log ft of ^{100}Tc, which they assumed to be equal to 4.2 for the reasons explained in section I. Griffiths and Vogel showed that the EC decay rate should have been more than a factor of six faster than that corresponding to $\log ft = 4.2$ in order to simultaneously explain all the β^- and the EC decay rates of ^{100}Tc. The fact that we obtain a $\log ft$ so close to the one they used, confirms the failure of the QRPA calculation to reproduce the measurements on ^{100}Mo.

IV. ACKNOWLEDGMENTS

We are very grateful to Wick Haxton for suggesting this measurement to us, to T.L. Khoo from ANL for lending us the NaI annulus and to D.A. Knapp from LLNL for lending us the Ge detector. One of us (A.G.) wishes to thank Stuart Freedman and Petr Vogel for very fruitful discussions. This work was supported by the Nuclear Physics Division of the U.S. Department of Energy under Contract DE-AC03-76SF00098, and Fundação de Amparo à Pesquisa do Estado de São Paulo, FAPESP, São Paulo, Brazil. M.M.H. acknowledges the support of the Nuclear Physics Division of the U.S. Department of Energy under Contract DE-FG05-87ER40314, and LBL during the summer of 1992.

†On leave from Instituto de Física, Universidade de São Paulo, Caixa Postal 20516, 01498 São Paulo, SP, Brasil.

‡On leave from R. Bošković Institute, Zagreb, Croatia.

REFERENCES

[1] W.C. Haxton and G.J. Stephenson, Jr., Prog. in Part. and Nucl. Phys., **12**, 409(1984).

[2] S.R. Elliott, *et al.*, J. Phys. G: Nucl. Part. Phys., **17**, S145(1991).

[3] H. Ejiri, *et al.*, J. Phys. G: Nucl. Part. Phys., **17**, S155(1991).

[4] F. Boehm and P. Vogel, *Physics of Massive Neutrinos*, Cambridge University Press, (1987).

[5] *Table of Isotopes*, C.M. Lederer and V.S. Shirley ed., (1978).

[6] J. Abad, A. Morales, R. Nuñez-Lagos, and A.F. Pacheco, An.Fis., **A80**, 9 (1984).

[7] *Table of Radioactive Isotopes*, E. Browne and R.B. Firestone, (1986).

[8] Y. Isozumi, Nucl. Inst. and Meth. in Phys. Res., **A280**, 151(1989).

[9] R.L. Watson, E.T. Chulick, and R.W. Howard, Phys. Rev. C, **6**, 2189(1972).

[10] H. Behrens and J. Jänecke, 'Numerical Tables for Beta-Decay and Electron-Capture', Landolt-Börnstein, New Series Vol. I/4, Springer, Berlin-Heidelberg-New York, (1969).

[11] T. Bernatowicz, *et al.*, Phys. Rev. Lett., **69**, 2341 (1992).

[12] J. Engel, P. Vogel, and M.R. Zirnbauer, Phys. Rev. C, **37**, 731(1988).

[13] A. Griffiths and P. Vogel, Phys. Rev. C, **46**, 181(1992).

[14] A.S. Barabash *et al.*, in *Massive Neutrino Tests of Fundamental Symmetries*, edited by O. Fackler and J. Tran Thanh Van (Edition Frontieres, Gif-sur-Yvette, 1991), p. 77.

FIGURES

FIG. 1. Decay scheme of ^{100}Tc. The goal of the present work is the determination of the log ft for the EC decay. All energies are given in keV.

FIG. 2. Schematic diagram of the experimental set-up. The radioactivity was deposited on a tape which was moved by a computer tape drive unit every 30 s. The counting station consisted of a Ge planar detector, surrounded by an annular NaI, and a plastic scintillator through which the tape was threaded. A second Ge detector was used to monitor longer lived contaminant radioactivity.

FIG. 3. a)Raw and plastic-plus-NaI vetoed Ge spectra. b)Low energy portion of the spectra shown in a).

FIG. 4. Fit to the low energy portion of the vetoed Ge spectrum.

FIG. 5. Gamma-ray detection efficiency vs. energy in the Ge detector. The arrows point to the data obtained with the ^{96}Tc source. The rest of the data was obtained with calibrated sources. The line shows the best fit to the calibrated sources data.

FIG. 6. Time dependence of contaminant γ-ray peak areas as counted using a source prepared by depositing radioactivity on a fixed tape during two hours. The fits were used to extrapolate the amount of contaminants present during our experiment.

FIG. 7. Total 'time' spectrum. The lines indicate the divisions that were used to obtain the gated energy spectra for the half-life measurement.

FIG. 8. a) χ^2 vs. half-life, obtained using the data shown above. b)Area of the Mo $K\alpha$ x-ray peak obtained on energy spectra gated as shown in the previous figure vs. time. The fit was done using a fixed constant term (corresponding to the contribution due to contaminants) plus an exponential with free amplitude and half-life. The line shows the fit corresponding to the minimum χ^2.

TABLES

TABLE I. Isotopic composition of Mo targets

Isotope	atomic percent
^{100}Mo	97.42 ± 0.03
^{98}Mo	0.96 ± 0.03
^{97}Mo	0.28 ± 0.03
^{96}Mo	0.34 ± 0.03
^{95}Mo	0.29 ± 0.03
^{94}Mo	0.18 ± 0.03
^{92}Mo	0.53 ± 0.03

TABLE II. Contribution of Tc contaminants to Mo x rays

Istp.	$t_{1/2}$ (h)	Flux [a] (s^{-1})	I(x) [b] (%)	A(x ray)/A(^{99}Tc) [c]	Fraction[d] unvetoed	A(x ray)[e]
$^{99}Tc^m$	6.02	9120 ± 180				
^{96}Tc	102.7	60 ± 160	56.5	$(3 \pm 8) \times 10^{-4}$	$1 \pm 2\%$	(0.3 ± 1.0)
$^{96}Tc^m$	0.858	300 ± 160	1.2	$(4.3 \pm 2.3) \times 10^{-3}$	$8 \pm 2\%$	(28 ± 16)
^{95}Tc	20.0	248 ± 10	56.5	$(7.2 \pm 0.3) \times 10^{-3}$	$25 \pm 4\%$	(147 ± 24)
$^{95}Tc^m$	1460	159 ± 82	55.9	$(6.2 \pm 3.2) \times 10^{-5}$	$21 \pm 4\%$	(1 ± 1)
^{94}Tc	4.88	19 ± 2	50.9	$(2.0 \pm 0.2) \times 10^{-3}$	$1 \pm 2\%$	(2 ± 4)
$^{94}Tc^m$	0.867	118 ± 10	16.9	$(2.4 \pm 0.2) \times 10^{-2}$	$18 \pm 4\%$	(352 ± 83)
^{93}Tc	2.75	43 ± 4	49.9	$(8.0 \pm 0.7) \times 10^{-3}$	$28 \pm 5\%$	(183 ± 36)
^{92}Tc	0.073	≤ 2 [f]	18.3		$4 \pm 2\%$	≤ 4
^{97}Nb	1.2	774 ± 50	0.2	$(1.3 \pm 0.1) \times 10^{-3}$	$22 \pm 5\%$	(24 ± 6)
^{96}Nb	23.4	≤ 10	0.6	$\leq 2.7 \times 10^{-6}$	$1 \pm 2\%$	$\leq 2 \times 10^{-3}$
^{95}Nb	840	≤ 243	0.1	$\leq 3.0 \times 10^{-7}$	$\leq 50\%$	$\leq 1 \times 10^{-2}$
^{94}Nb	1.7×10^8	$\leq 5 \times 10^7$	0.2	$\leq 5.1 \times 10^{-7}$	$\leq 10\%$	$\leq 4 \times 10^{-3}$
Total						737 ± 95

[a]Calculated from the 24 hours counting of the 2-hour-source; except for ^{92}Tc.

[b]Probability of emission of a Mo $K\alpha$ x ray per decay (from ref. [7]). The uncertainties are neglected.

[c]Deduced ratio of Mo $K\alpha$ x rays to ^{99}Tc 140.5 keV γ-rays in our experiment.

[d]Fraction of contaminant decays that escape the NaI veto, calculated using the measured NaI or plastic scintillator veto efficiency. This number is determined by the NaI efficiency for the Tc isotopes, and mainly by the plastic detector efficiency for the Nb isotopes. In the cases where there are EC decays to several daughter states, we quote a number which multiplied by the x-ray intensity in column 4 gives the percentage of decays which emit a $K\alpha$ x ray and escape the NaI vetoing.

[e]Contribution to the area of the Mo $K\alpha$ x-ray peak in the vetoed spectrum.

[f]This limit was placed by looking at characteristic γ rays in the spectrum of the second Ge spectrum.

TABLE III. Ratio of raw/NaI-vetoed peak areas

	Ru x ray	540 keV	591 keV
R	1.8 ± 0.3	5.5 ± 0.7	7.4 ± 0.7

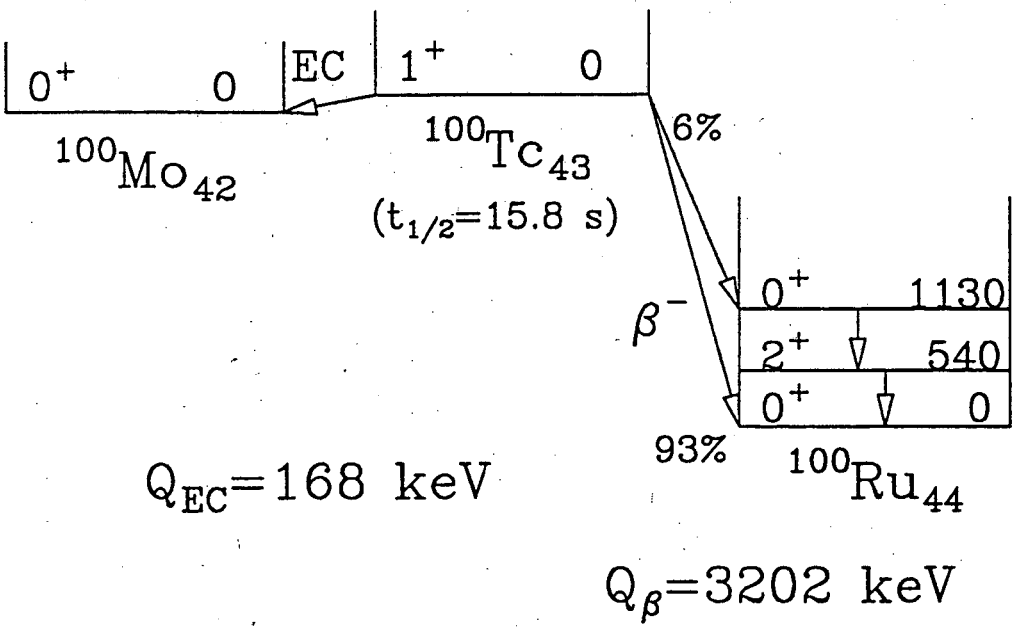

Fig. 1 of 'Electron-Capture Decay of ^{100}Tc...', by A.García et al.

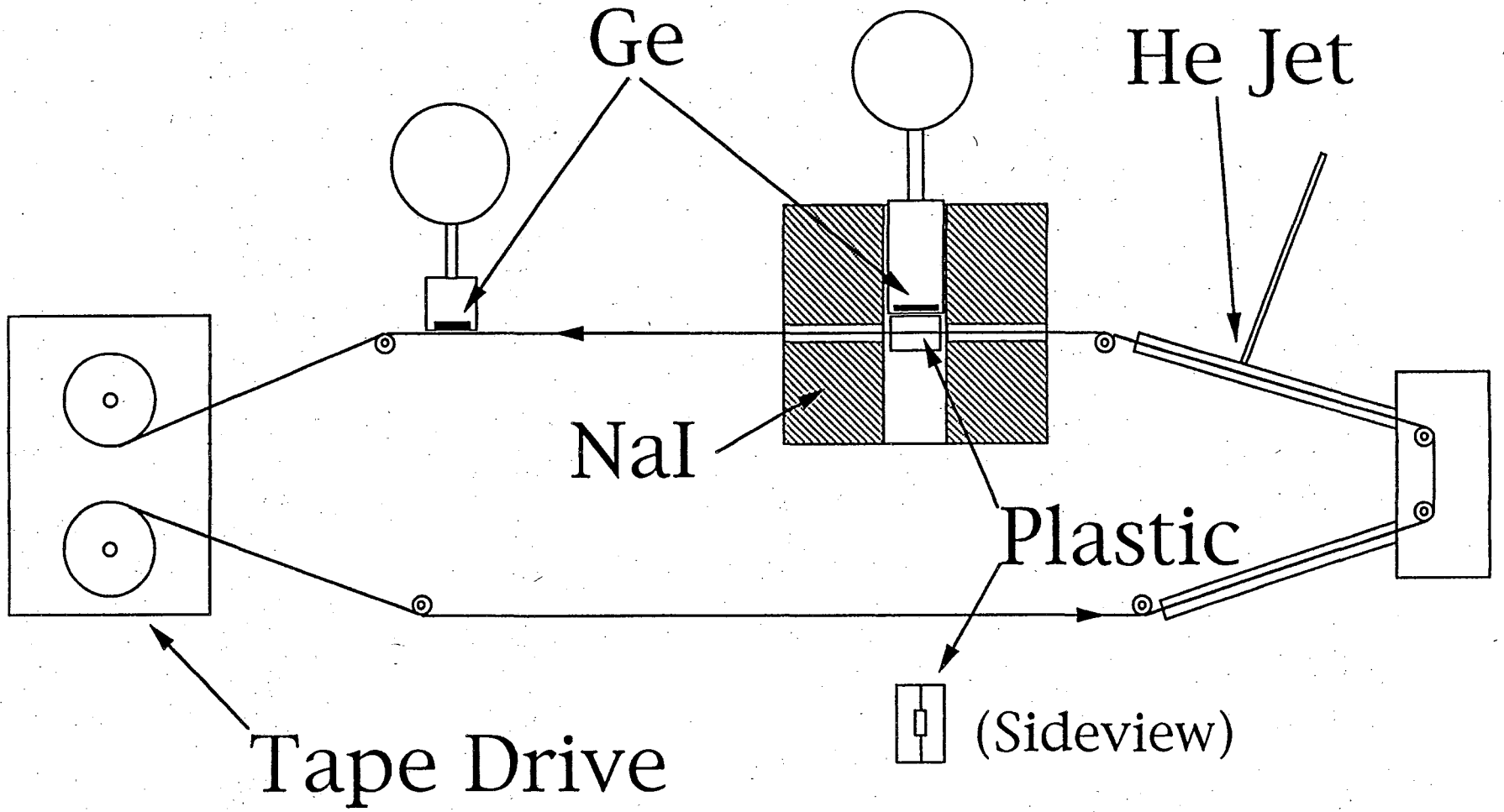

Fig. 2 of 'Electron-Capture Decay of ^{100}Tc...', by A.García et al.

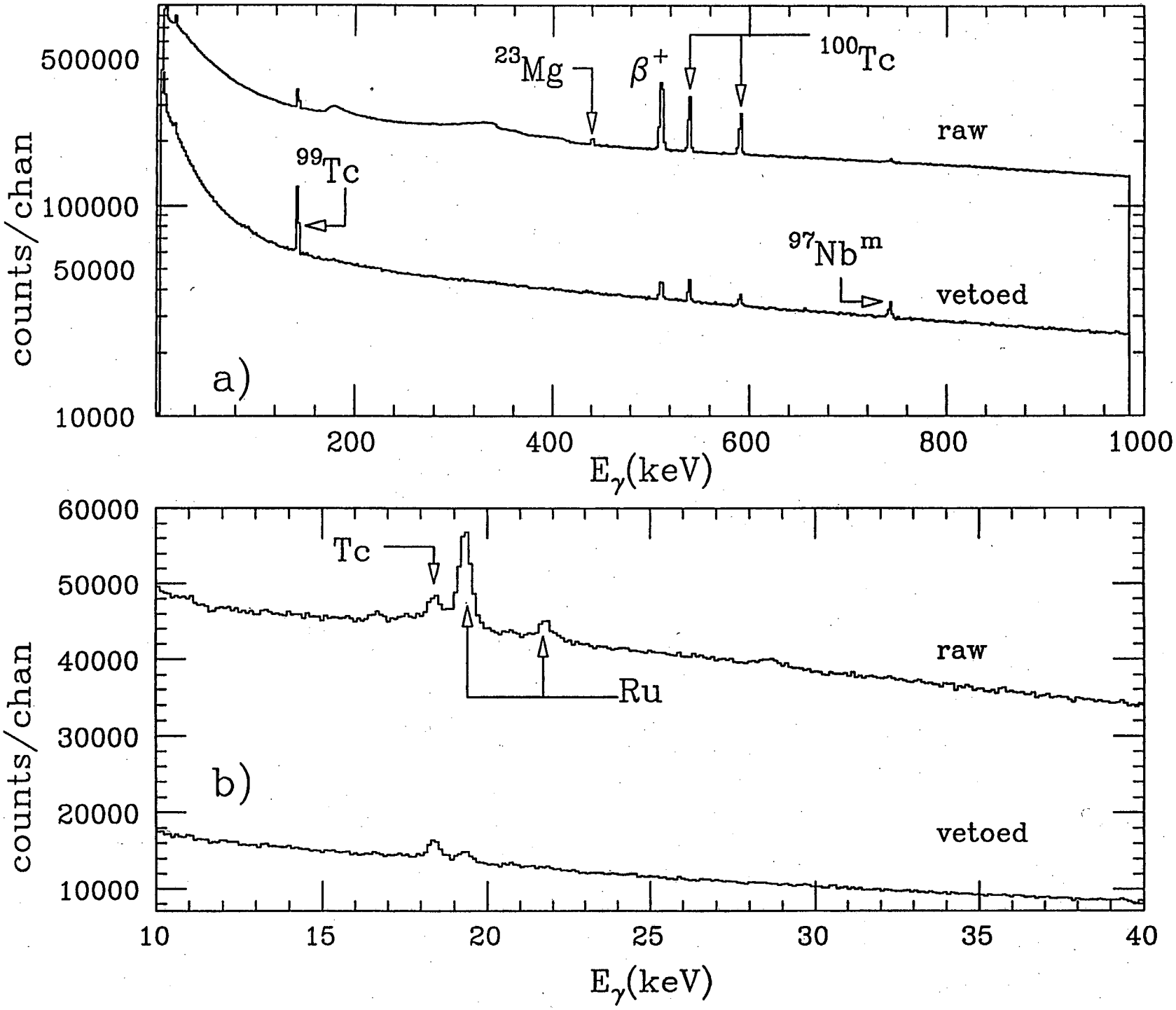

Fig. 3 of 'Electron-Capture Decay of ^{100}Tc...', by A.García et al.

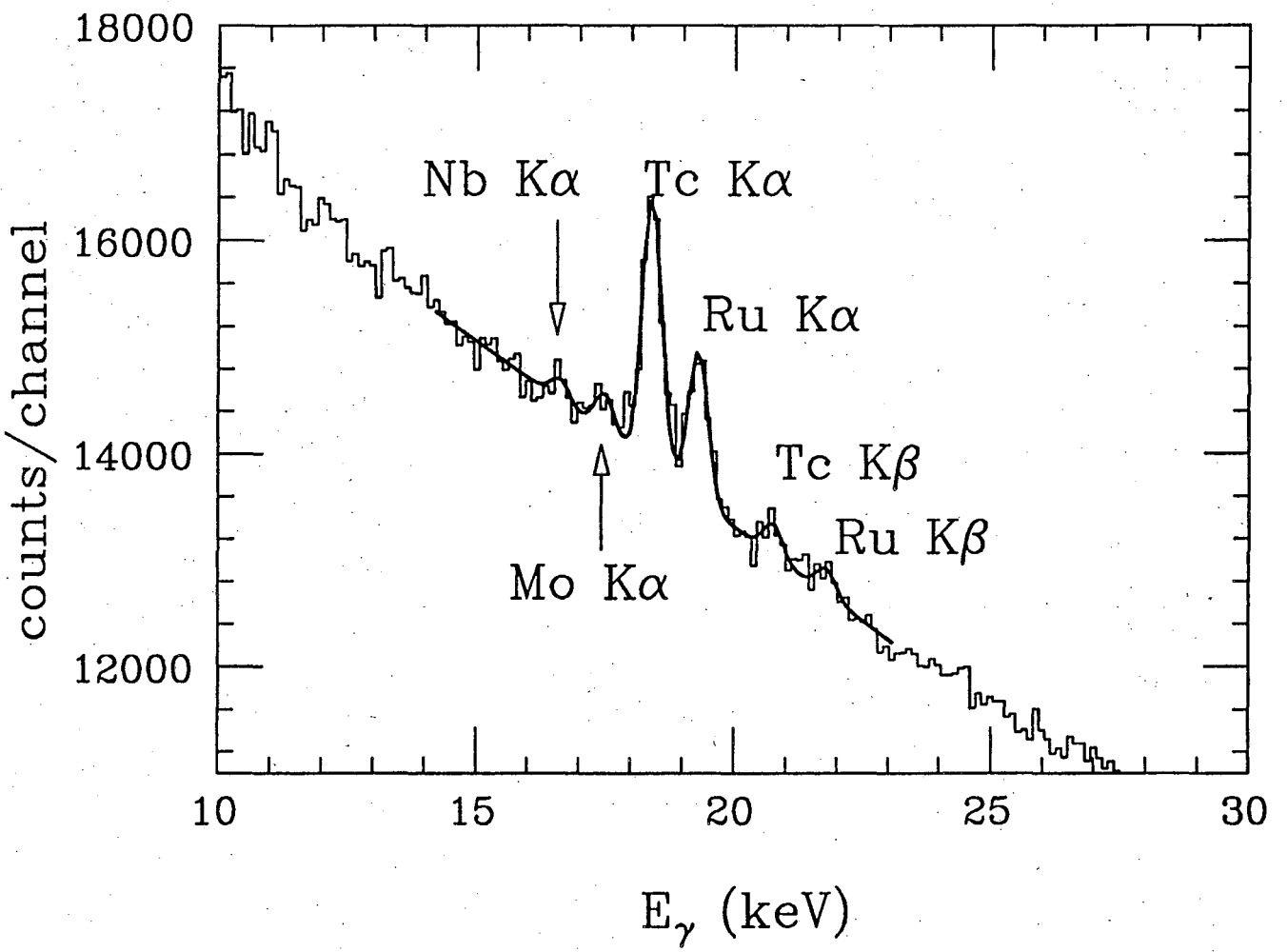

Fig. 4 of 'Electron-Capture Decay of ^{100}Tc...', by A.García et al.

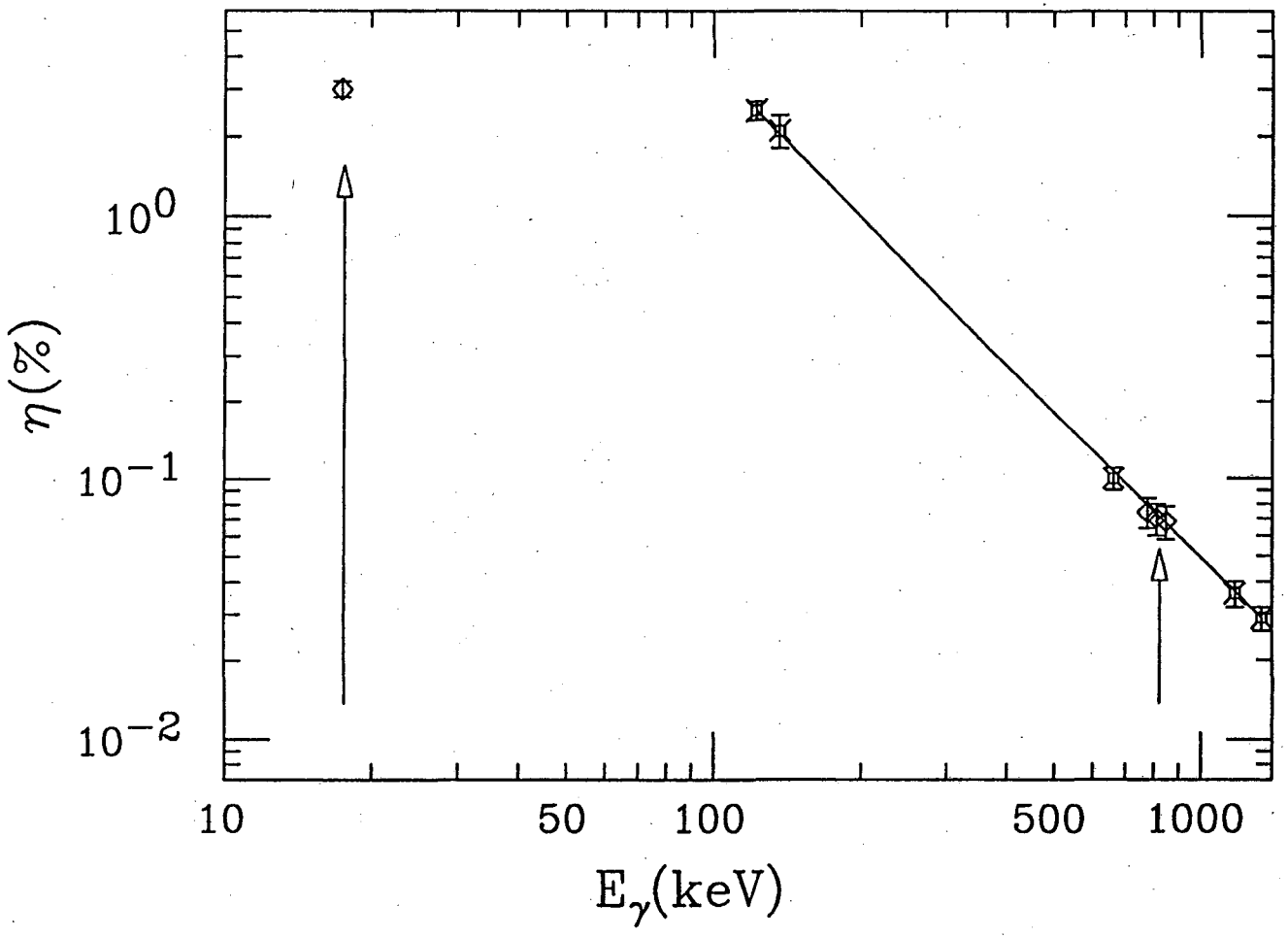

Fig. 5 of 'Electron-Capture Decay of ^{100}Tc...', by A.García et al.

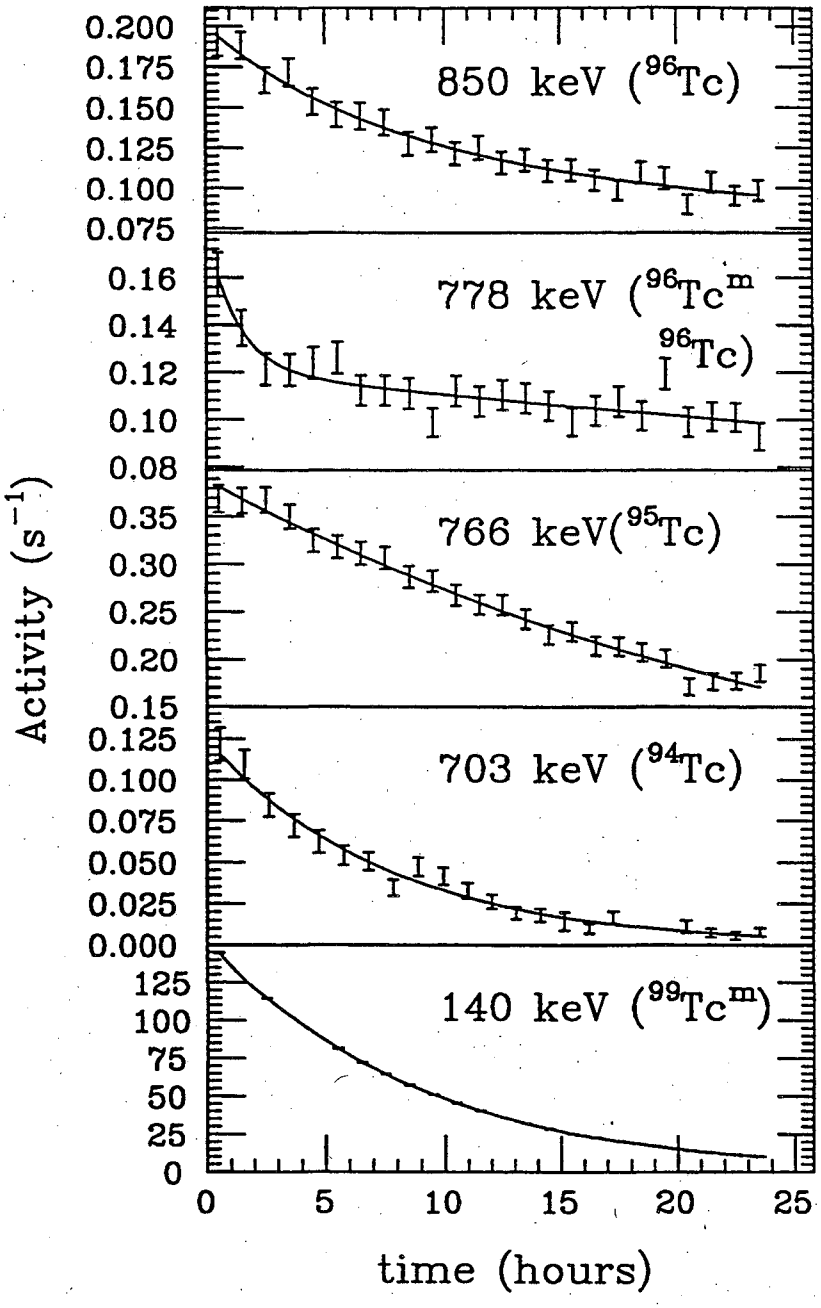

Fig. 6 of 'Electron-Capture Decay of ^{100}Tc...', by A.García et al.

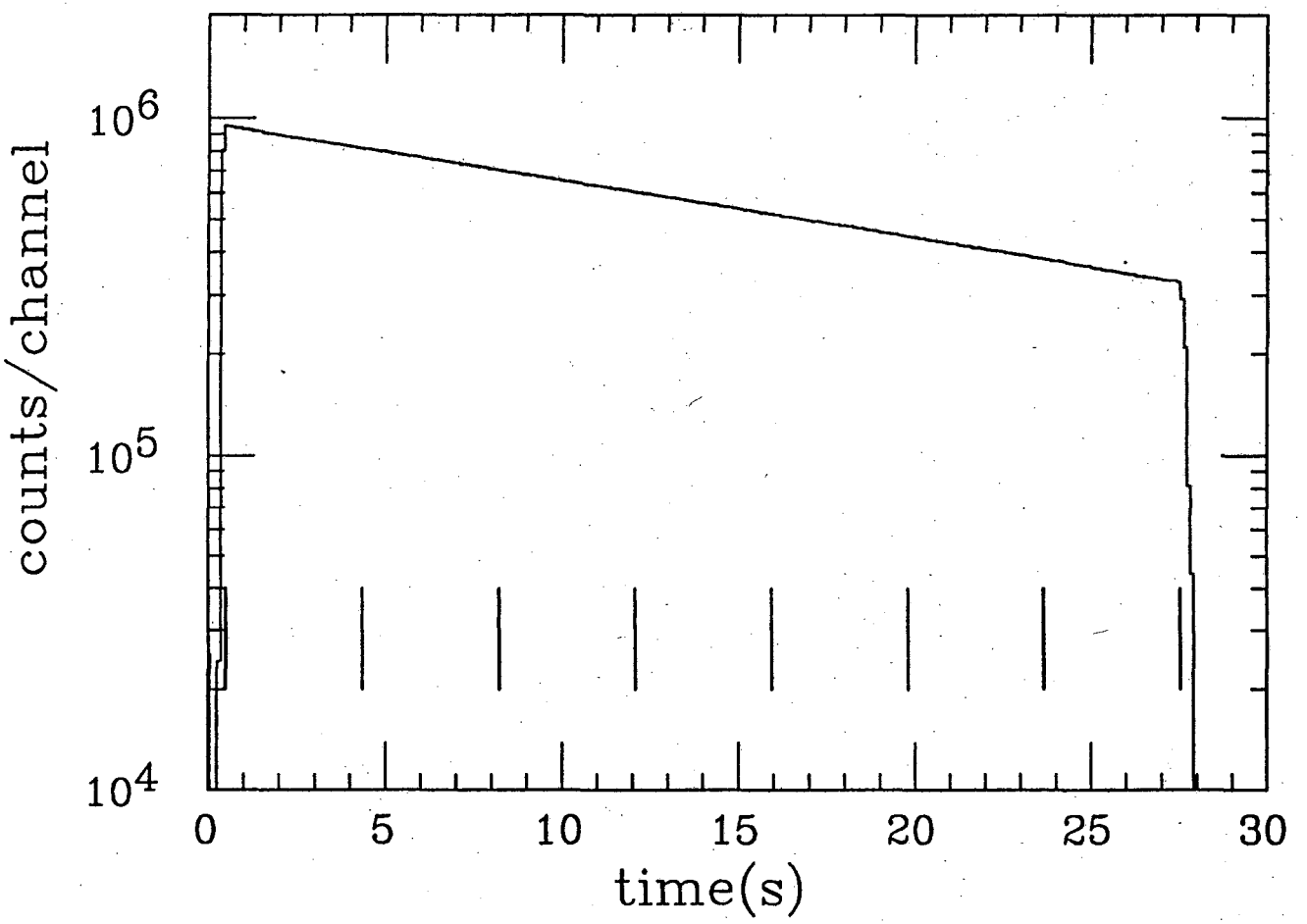

Fig. 7 of 'Electron-Capture Decay of ^{100}Tc...', by A.García et al.

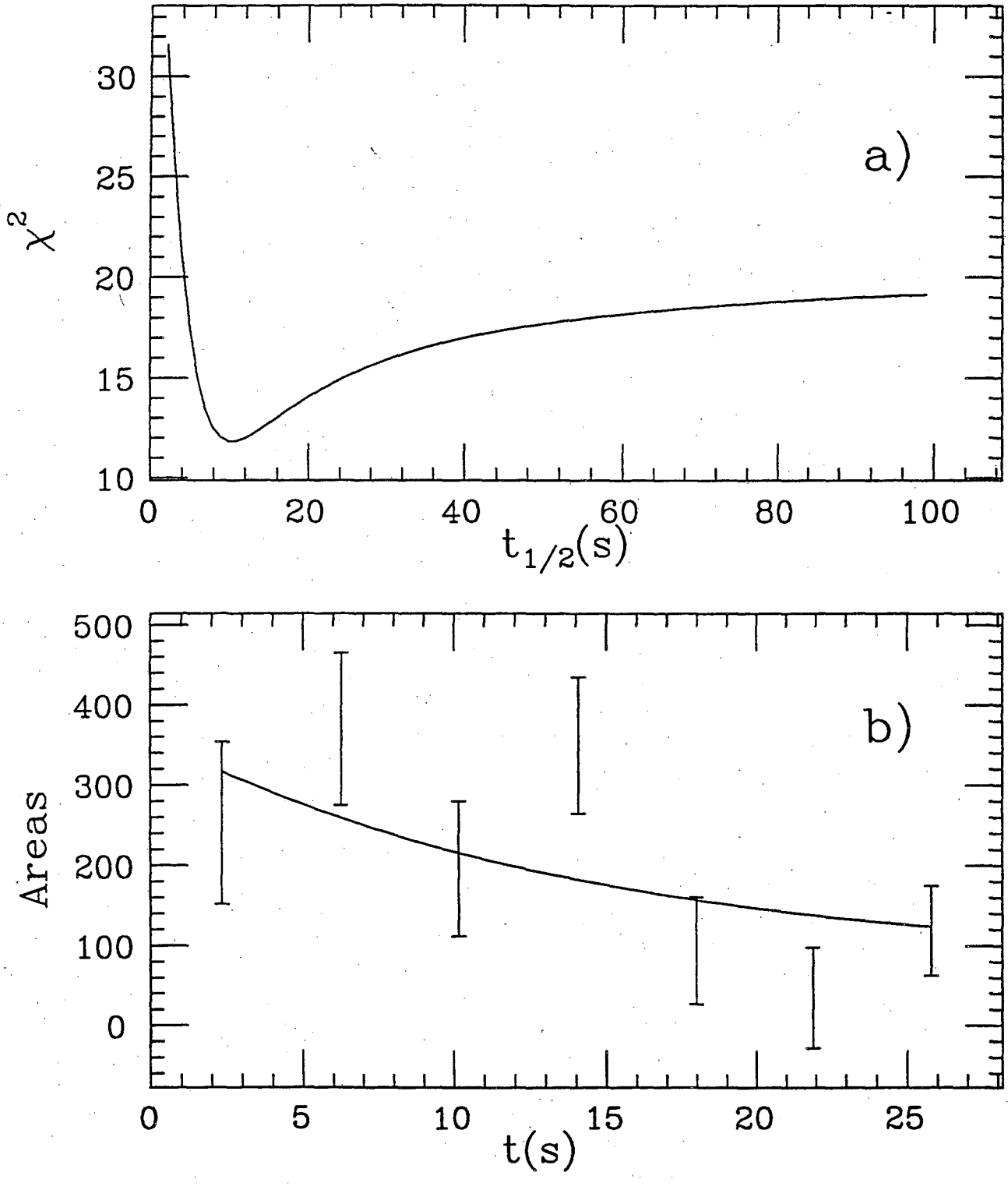

Fig. 8 of 'Electron-Capture Decay of ^{100}Tc...', by A.García et al.

LAWRENCE BERKELEY LABORATORY
UNIVERSITY OF CALIFORNIA
TECHNICAL INFORMATION DEPARTMENT
BERKELEY, CALIFORNIA 94720